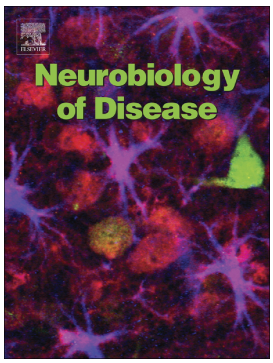

Cerebellar alterations in a model of Down syndrome: The role of the Dyrk1A gene

Susana García-Cerro, Verónica Vidal, Sara Lantigua, Maria Teresa Berciano, Miguel Lafarga, Pedro Ramos-Cabrer, Daniel Padro, Noemí Rueda, Carmen Martínez-Cué

PII: S0969-9961(17)30280-2
DOI: doi:10.1016/j.nbd.2017.12.002
Reference: YNBDI 4074

To appear in: *Neurobiology of Disease*

Received date: 19 September 2017
Revised date: 13 November 2017
Accepted date: 4 December 2017

Please cite this article as: Susana García-Cerro, Verónica Vidal, Sara Lantigua, Maria Teresa Berciano, Miguel Lafarga, Pedro Ramos-Cabrer, Daniel Padro, Noemí Rueda, Carmen Martínez-Cué , Cerebellar alterations in a model of Down syndrome: The role of the Dyrk1A gene. The address for the corresponding author was captured as affiliation for all authors. Please check if appropriate. Ynbdi(2017), doi:10.1016/j.nbd.2017.12.002

Cerebellar alterations in a model of Down syndrome: the role of the *Dyrk1A* gene

Susana García-Cerro[1], Verónica Vidal[1], Sara Lantigua[1], Maria Teresa Berciano[2], Miguel Lafarga[2], Pedro Ramos-Cabrer[3,4], Daniel Padro[3], Noemí Rueda[1], Carmen Martínez-Cué[1*]

[1] Department of Physiology and Pharmacology, Faculty of Medicine, University of Cantabria, Santander, 39011, Spain

[2] Department of Anatomy and Cell Biology and CIBERNED, University of Cantabria-IDIVAL, Santander, 39011, Spain

[3] Molecular Imaging Unit, CIC BiomaGUNE, Donostia-San Sebastian, 20009, Spain

[4] Ikerbasque, The Basque Foundation for Science, Bilbao, 48013, Spain

***Corresponding author:** email: martinec@unican.es

Department of Physiology and Pharmacology, Faculty of Medicine, University of Cantabria, Santander, 39011, Spain

SG-C current affiliation: Department of Clinical Foundations, Pharmacology Unit, Faculty of Medicine, University of Barcelona, Barcelona, 08036, Spain

ABSTRACT

Down syndrome (DS) is characterized by a marked reduction in the size of the brain and cerebellum. These changes play an important role in the motor alterations and cognitive disabilities observed in this condition. The Ts65Dn (TS) mouse, the most commonly used model of DS, reflects many DS phenotypes, including alterations in cerebellar morphology. One of the genes that is overexpressed in both individuals with DS and TS mice is *DYRK1A/Dyrk1A* (dual-specificity tyrosine-(Y)-phosphorylation regulated kinase 1A), which has been implicated in the altered cerebellar structural and functional phenotypes observed in both populations. The aim of this study was to evaluate the effect of *Dyrk1A* on different alterations observed in the cerebellum of TS animals. TS mice were crossed with *Dyrk1A* +/- KO mice to obtain mice with a triplicate segment of Mmu16 that included *Dyrk1A* (TS +/+/+), mice with triplicate copies of the same genes that carried only two copies of *Dyrk1A* (TS +/+/-), euploid mice that expressed a normal dose of *Dyrk1A* (CO +/+) and CO animals with a single copy of *Dyrk1A* (CO +/-). Male mice were used for all experiments. The normalization of the *Dyrk1A* gene dosage did not rescue the reduced cerebellar volume. However, it increased the size of the granular and molecular layers, the densities of granular and Purkinje cells, and dendritic arborization. Furthermore, it improved the excitatory/inhibitory balance and walking pattern of TS +/+/- mice. These results support the hypothesis that *Dyrk1A* is involved in some of the structural and functional cerebellar phenotypes observed in the TS mouse model.

Keywords: Down syndrome, cerebellum, Ts65Dn, *Dyrk1A*

Highlights:

Dyrk1A is implicated in cerebellar alterations in a model of Down syndrome.

Normalization of the *Dyrk1A* dosage rescues granular and Purkinje cell densities in trisomic mice.

Normalization of the *Dyrk1A* dosage rescues the size of the granular and molecular layers.

Dyrk1A is implicated in the excitatory/inhibitory balance in a model of Down syndrome.

INTRODUCTION

Down syndrome (DS) is characterized by several structural and functional abnormalities in the central nervous system, and a reduction in brain size is one of the most important characteristics of this condition. Additionally, an even greater reduction in cerebellar volume is observed in fetuses, newborns, children and adults with DS. In these individuals, both the total volume and the sizes of specific cerebellar cortical structures, such as the internal granule layer (IGL) and molecular layer (ML), are also markedly smaller (Aylward et al., 1997; Rotmensch et al., 1997; Baxter et al., 2000; Winter et al., 2000; Guidi et al., 2011). These morphological alterations are likely caused by a decrease in the densities of cerebellar granule cells (GC) and Purkinje cells (Baxter et al., 2000; Guidi et al., 2011).

Traditionally, the cerebellum has been regarded as a key regulator of motor control and motor learning (Palay and Chan-Palay, 1982). Children and adults with DS display fine motor deficits that have been attributed to cerebellar dysfunction (Latash and Corcos, 1991; Latash et al., 2002). However, based on accumulating evidence, the cerebellum is implicated in higher cognitive functions (Hilber et al., 1998; Petrosini et al., 1998; Rondi-Reig and Burguière, 2005; Galiano et al., 2013; Rochefort et al. 2013). Because cognitive disabilities are a major hallmark of DS, the altered neuroanatomy of the cerebellum in individuals with DS may also be partially responsible for the observed cognitive deficits.

Several murine models of DS present similar abnormalities in the cerebellum, beginning at early postnatal ages. The Ts65Dn (TS) mouse carries a triplication of the distal end of Mmu16, extending from the *Mrp139* to the *Znf295* genes (Sturgeon and Gardiner, 2011). TS mice have a smaller cerebellum, vermis, GL and ML, and less dense GC and Purkinje cell populations (Baxter et al., 2000; Roper et al., 2006; Necchi et al., 2008; Contestabile et al., 2009). Other murine models of DS, such as the Ts1Cje mouse, which is caused by trisomy of the Mmu16 region from *Sod1* to *Znf295* (Sago et al., 1998), and the Tc1 model, in which all of Hsa21 is triplicated, also have a smaller cerebellum and a less dense GC population (Olson et al., 2004; O'Doherty et al., 2005).

Because different murine models of DS and individuals with DS share similar cerebellar anomalies, the triplication of this set of orthologous genes might be responsible for these phenotypes. Several candidate Hsa21 genes have been reported to play roles in brain development**.** One of these genes is *DYRK1A* (dual-specificity tyrosine-(Y)-phosphorylation regulated kinase 1A), which encodes a protein kinase that has crucial

functions during brain development and in adult brain physiology (Becker and Sipple, 2011; Tejedor and Hämmerle, 2011). *DYRK1A* is important for normal brain growth in both mice and humans (Fotaki et al., 2002; Moeller et al., 2008; van Bon et al., 2011; Guedj et al., 2012). This gene is expressed at high levels in the cerebellum (Martí et al., 2003), and murine models with altered *Dyrk1A* expression exhibit altered motor abilities (Altafaj et al., 2001; Martínez de Lagrán et al., 2004; Fotaki et al., 2002, 2004; Souchet et al., 2014).

The aim of this study was to evaluate the role of the *Dyrk1A* gene in the various morphological alterations that occur in the cerebellum of the TS model of DS. TS mice were crossed with *Dyrk1A* KO mice to obtain mice with a triplicated segment of Mmu16 that included *Dyrk1A* (TS +/+/+), mice that were trisomic but carried only two copies of *Dyrk1A* (TS +/+/-), euploid (CO) mice that expressed a normal dose of *Dyrk1A* (CO +/+) and CO animals with a single copy of *Dyrk1A* (CO +/-). Cerebellar volume, sizes of the GL and ML, GC and Purkinje cell densities, dendritic arborization, and the walking patterns of each group of mice were assessed.

METHODS

1. Experimental animals

Mice were generated by repeatedly backcrossing B6EiC3Sn a/A-Ts(17<16>)65Dn (TS) females with C57BL/6Ei x C3H/HeSNJ (B6EiCSn) F1 hybrid males. The Robertsonian Chromosome Resource (The Jackson Laboratory, Bar Harbor, ME, USA) provided the parental generations, and animals were mated at the animal facilities of the University of Cantabria.

TS females were crossed with *Dyrk1A*+/- heterozygous male mice on a mixed C57BL/6-129Ola genetic background (Fotaki et al., 2002) to obtain the following groups of mice: i) mice carrying a triplicated Mmu16 segment (TS +/+/+) extending from the *Mrp139* gene to the *Znf295* gene, which includes the *Dyrk1A* gene; ii) mice trisomic for all of these genes but diploid for *Dyrk1A* (TS +/+/-); iii) euploid (CO) mice with a normal *Dyrk1A* dosage (CO +/+) and iv) CO animals with a single copy of *Dyrk1A* (CO +/-).

To determine trisomy, animals were karyotyped using real-time quantitative PCR (qPCR), as previously described (Liu et al., 2003). C3H/HeSnJ mice carry a recessive mutation that leads to retinal degeneration (Rd). Hence, all animals were genotyped using standard PCR to detect the *Rd* mutation (Bowes et al., 1993). Experiments were performed using wt/wt or *Rd1*/wt animals. The *Dyrk1A* +/- mice were genotyped using PCR, as previously described (Fotaki et al., 2002).

Ninety-six male mice were used. Ten animals (6-10 months old) from each group were tested in the MRI studies, and fourteen mice (5-6 months old) in each group were used in the remaining experiments. Eight animals from each group were used to i) immunohistochemically visualize Purkinje cell arborization, ii) quantify GC and Purkinje cell densities, iii) determine the density of glutamatergic and GABAergic synapse markers, and iv) perform the footprint study. Six animals from each group were used for the western blot analysis of Dyrk1A protein levels. The researchers were blinded to the genotypes and karyotypes of the animals throughout the experiments.

2. Western blot analysis

Mice were euthanized by decapitation, and the cerebellum was dissected. Whole-tissue lysates of the cerebellum were prepared using a previously described method (García-Cerro et al., 2014). The total protein content of each sample was determined using the method described by Lowry et al. (1951). An identical amount of total protein (50 µg) from each sample was loaded onto a 10% sodium dodecyl sulfate-polyacrylamide gel, electrophoresed, and transferred to a polyvinylidene difluoride

(PVDF) membrane (Bio-Rad, Hercules, CA, USA) using a Mini Trans-Blot Electrophoresis Transfer Cell (Bio-Rad). The efficient transfer of proteins was confirmed by staining the PVDF membrane with Ponceau red (Sigma-Aldrich, St. Louis, MO, USA). Non-specific binding of antibodies was prevented by incubating the membranes with TBST buffer (10 mM Tris-HCl, pH 7.6, 150 mM NaCl, and 0.05% Tween 20) containing 3% bovine serum albumin (BSA). Blots were incubated with a mouse monoclonal anti-DYRK1A antibody (1:250; Abnova Corporation, Taipei, Taiwan, ROC) diluted in TBST containing 3% BSA overnight at 4 °C. After the membrane was extensively washed with TBST, it was incubated with a goat anti-mouse IRDye 800CW antibody (1:10,000; LI-COR Biotechnology, Lincoln, Nebraska, USA) for 1 h at room temperature. The resulting fluorescence was detected using a LI-COR ODYSSEY IR Imaging System V3.0 (LI-COR Biotechnology). Images were exported and saved as gray scale TIFF files (16 bit) to improve the contrast between signal and noise. The integrated optical density of the bands was subsequently determined using ImageJ NIH software (http://rsb.info.nih.gov/ij) and normalized to the background values. The relative variations between the bands among the four groups of experimental mice were calculated in the same experiment. Each individual sample was evaluated in at least three independent experiments. Values were within a linear range. Blots were reprobed using a mouse monoclonal anti-GAPDH antibody (6C5) (1:2,000; Santa Cruz Biotechnology, Santa Cruz, CA, USA) to ensure equal loading.

3. Cerebellar volume (MRI)

Mice were euthanized and their brains were fixed using transcardial perfusion with saline followed by 4% paraformaldehyde.

MRI studies were performed using a Biospec USR7/30 spectrometer (Bruker, Ettlingen, Germany) with a 7-Tesla 30-cm bore magnet equipped with a 12-cm gradient insert capable of switching 400 mT/m in 90 ms.

A 40-mm birdcage 1H-resonator was used for RF transmission and reception. Imaging experiments were performed on extracted brains that were placed in 2-ml syringes filled with 1X PBS (phosphate-buffered saline) to avoid susceptibility effects at tissue/air interfaces.

Following the automatic calibration of the system (i.e., pulse power, shim, and resonance frequency) and the acquisition of a multi-planar scout image (Gradient echo), which was used as a localizer to correctly position the imaging planes, 3D images were acquired using a high-resolution RARE (rapid acquisition with relaxation

enhancement) pulse sequence with the following parameters: the field of view (FOV), 20 x 12 x 8.6 mm^3, and image matrix, 200 x 120 x 86 points, yielding an isotropic pixel resolution of 0.100 x 0.100 x 0.100 mm^3/pixel; effective bandwidth, 50 kHz, RARE factor, 12; effective echo time, 63 ms (TE = 10.5 ms); repetition time, 1700 ms and number or averages, 6. The total acquisition time was 2 h 26 minutes. Image post-processing procedures and analyses were performed using ImageJ software.

4. Histological and staining procedures

Animals were deeply anesthetized with pentobarbital and transcardially perfused with saline followed by 4% paraformaldehyde in PBS. Subsequently, the brains were post-fixed with the same fixative overnight at 4 °C, cryoprotected in 30% sucrose and frozen in dry ice. The brains were cut in the sagittal plane into 30-µm-thick (cryostat) free-floating sections for immunolabeling of glutamatergic and GABAergic synapse markers. For the remaining experiments, 5-µm-thick sections were collected on microscope slides. Tissue sections were stored at -20 °C.

In all immunohistochemical studies, appropriate minimal positive and negative controls were used to avoid inaccurate conclusions about false-positive or false-negative results. As negative controls for immunostaining, assays were performed using a similar protocol, with the exception that primary antibodies were omitted. For positive controls, the specificity of antibodies was previously validated by western blot experiments showing the recognition of specific bands corresponding to the proteins examined in our study.

5. Propidium iodide and DAPI staining

Tissue sections were incubated at room temperature, and the zone of interest was marked using a hydrophobic marker. Next, sections were washed with 1X PBS twice for 5 minutes each, treated with PBS-Tw (0.05%) for 5 minutes, dried and placed in a humid and dark chamber. Tissue sections were then incubated with DAPI (4'6-diamidino-2-phenylindole), a cytochemical marker of DNA, in PBS for 12 minutes to stain cell nuclei. Next, sections were washed three times with PBS for 5 minutes each. Purkinje cells were counterstained with propidium iodide (PI, dilution 1:2,000) for 20 minutes. Then, sections were washed with PBS and mounted with Vectashield anti-fade medium (Vector Laboratories, Peterborough, UK).

6. Area of the vermis, thickness of the GL and ML and length of the Purkinje cell layer

We obtained optical micrographs of DAPI-stained sagittal sections of the cerebellar vermis using a 5x objective (Leica DM6000 M, Leica Microsystems, Wetzlar, Germany) to estimate the different areas and lengths of regions of interest. This microscope automatically created single panoramic images of the cerebellum from each animal with which the different morphometric calculations were performed.

The mean thicknesses of the GL and the ML were calculated by dividing the length of each layer in a midline sagittal section by the total area of the layer. The Purkinje cell layer was included in the estimate of the thickness of the ML. Because a stereological technique was not used, changes in the parameters between groups are expressed as a percentage difference vs. the CO +/+ group, as previously described (Baxter et al., 2000).

7. Quantification of granule cell density

Granule cells were counted in 5-μm-thick sections of the GL stained with DAPI. Six sagittal sections of the cerebellar vermis were serially collected on glass slides. GL micrographs were recorded using a fluorescence microscope (Zeiss Axioskop 2 plus) under a 62x oil objective. Cells were counted within a 5,000-μm^2 area. Eight independent and non-overlapping fields were randomly selected along the length of folias IV, V, VI and VII in the cerebellum of each animal, and the number of GCs in each field were counted. The Abercrombie correction factor (Abercombrie, 1946) was used to correct the estimates by applying the following formula:

$$P = A [M / (L + M)]$$

where P is the final estimate of the cell number, A is the number of nuclei counted, M is the thickness of the section in μm, and L is the mean nuclear diameter (also in μm). Eight nuclei were randomly selected from each animal to estimate the nuclear diameter.

8. Quantification of Purkinje cell density

The total number of cells stained with PI in a complete midline sagittal section was counted and divided by the length of the Purkinje layer for each animal to determine the linear density of Purkinje cells.

9. Purkinje cell arborization

We used calbindin immunohistochemistry to evaluate the dendritic arborization in Purkinje cells in the ML of the cerebellum. Briefly, 5-µm-thick sections of the vermis were collected from animals in each experimental group and placed on SuperFrost Plus microscope slides (ThermoFisher Scientific), washed with PBS (3 x 10 minutes) and incubated with blocking agent (5% fetal bovine serum and 0.1% Triton X-100 in PBS) for 1 h at RT. Then, tissue sections were incubated with the primary rabbit polyclonal anti-calbindin antibodies (Swant, Switzerland 1:7,000 in the blocking agent) overnight at 4 °C, washed with 0.05% Tween 20 in PBS, incubated with the anti-rabbit secondary antibodies (conjugated to Alexa Fluor 488, Life Technologies, 1:75) for 1 h at RT, washed with PBS, and mounted with Vectashield-DAPI anti-fade medium (Vector Laboratories).

For each animal, a minimum of three regions of the ML of the cerebellar vermis were recorded using a Leica SP5 confocal microscope (Leica Microsystem, Wetzlar, Germany) with a 40x objective. Purkinje cell arborization was quantified using a systematic random design of dissector counting frames (100 x 100 μm^2). Three independent fields were randomly selected along the cerebellar vermis. The intensity of calbindin immunoreactivity was measured using ImageJ software. First, images obtained under the microscope were transformed to 16-bit images and calibrated, and background staining was then subtracted. Later, images were transformed to 32-bit images and normalized to obtain a gray scale value within the range of 0 to 1, where 0 represents white and 1 represents black. The mean gray values were measured within each frame and averaged to calculate the density for each animal.

10. Density of glutamatergic and GABAergic synapse markers (VGluT1 and VGAT immunofluorescence, respectively)

Free-floating, 30-µm sections of the cerebellar vermis were used to determine the density of GABAergic and glutamatergic synapse markers. Sections were first incubated with PBTBSA, and double immunohistochemistry was then performed. Glutamatergic and GABAergic boutons were immunolabeled using a guinea pig anti-vesicular glutamate transporter 1 antibody (VGluT1, 1:2,500; Millipore, Billerica, MA, USA) and an anti-GABA vesicular transporter antibody (VGAT, 1:100; Santa Cruz Biotechnology, Dallas, TX, USA), respectively. Then, tissue sections were incubated with the following secondary antibodies: Alexa Fluor 488-conjugated goat anti-guinea pig (1:1,000; Invitrogen, Carlsbad, CA, USA) and Alexa Fluor 594-conjugated donkey anti-goat (1:1,000; Invitrogen).

Immunolabeled synaptic boutons were measured in images obtained under a confocal microscope (Leica SP5). Four sections per animal were used to measure each synapse marker, and one random cerebellar area per section was measured. Images were analyzed using ImageJ software, as previously described (Martínez-Cué et al., 2013). Briefly, boutons positive for either VGluT1 or VGAT (because these markers are never co-localized) were measured separately. The same threshold was applied to all images. Images were converted to grey scale to improve the contrast between signal and noise. The area inside of a reference circle with a standard size of 325 μm^2 was measured. The reference space was located in the inner ML next to the Purkinje cell layer. The percentage of the reference area that was occupied by VGluT1- and VGAT-positive boutons and the excitatory-inhibitory ratio (VGluT1/VGAT) were calculated.

11. Footprint analysis

Footprint tests were used to evaluate the walking patterns of the different groups of mice, according to the protocol described by Martínez de Lagrán et al. (2004). Black waterproof ink was applied to the hind paws of each individual mouse. The animals were then placed at one end of a long, narrow tunnel (10 cm x 10 cm x 70 cm), which they spontaneously entered. A clean sheet of white paper (50 cm) was placed on the floor of the tunnel to record their footprints. Footprints located in the first and last 15 cm of the sheet were excluded from the analysis to discard possible artifacts that are unrelated to motor behavior. Each animal repeated the task three times, resulting in clear footprints on 20 cm of sheet. The average length and width between the paw prints and the number of strides per trial were measured. The coefficient of variation was calculated as the ratio between the standard deviation and the mean value of five consecutive strides with the left paw.

12. Experimental design and statistical analysis

All data were analyzed using a two-way (‘karyotype’ x ‘*Dyrk1A*’) ANOVA. The mean values for each experimental group were compared using Bonferroni’s post hoc tests when all groups were compared and Student’s t-test when two groups were compared. All analyses were performed using SPSS for Windows version 22.0 (Armonk, New York, USA).

RESULTS

1. Levels of the Dyrk1A protein in the cerebellum are correlated with the dose of the *Dyrk1A* gene

First, we determined the levels of the Dyrk1A protein in the cerebellum of each experimental group to evaluate whether its expression levels correlated with the *Dyrk1A* gene dosage. As expected, a western blot analysis of cerebellar lysates revealed a direct correlation between Dyrk1A protein levels and the number of *Dyrk1A* gene copies the animal carried. Thus, TS +/+/+ animals had higher levels of this protein than the CO +/+ mice (ANOVA 'karyotype': $F_{(1,20)} = 22.73$, $p < 0.001$; **figure 1**). When the number of functional copies of *Dyrk1A* was reduced by one, the levels of this protein were normalized in TS +/+/- animals and reduced in CO +/- animals ('*Dyrk1A*': $F_{(1,20)} = 11.92$, $p = 0.003$; 'karyotype x *Dyrk1A*': $F_{(1,20)} = 0.61$, $p = 0.44$; **figure 1**).

2. Knockout of one copy of the *Dyrk1A* gene reduced the cerebellar volume of CO +/- mice, but not of TS +/+/- mice

When the effect of 'karyotype' on cerebellar volume was analyzed, we did not observe significant differences between the two groups of TS mice and the two groups of CO mice (ANOVA 'karyotype': $F_{(1,36)} = 3.01$, $p = 0.092$). However, this finding was probably because although the CO +/- mice had a lower cerebellar volume (ANOVA '*Dyrk1A*': $F_{(1,36)} = 12.86$, $p < 0.001$) than the TS +/+/+ mice (TS +/+/+ vs. CO +/+, $t = 7.26$, $p < 0.001$; **figure 2**). In fact, knockout of a functional copy of the *Dyrk1A* gene reduced the cerebellar volume of the CO +/- mice, but had no effect on the TS +/+/- animals (ANOVA 'karyotype x *Dyrk1A*': $F_{(1,36)} = 42.86$, $p < 0.001$).

3. Reducing the *Dyrk1A* gene dosage normalized the size of the cerebellar vermis in TS +/+/- mice

TS +/+/+ mice presented a marked reduction in cerebellar size (12.9% smaller than the CO +/+ mice, **figure 3**), but the normalization of the *Dyrk1A* dosage completely rescued this alteration, as shown in the TS +/+/- mice, in which the cerebellar size was similar to the CO +/+ group (MANOVA 'karyotype' $F_{(1,28)} = 0.02$, $p = 0.889$; '*Dyrk1A*' $F_{(1,28)} = 0.155$. $p = 0.697$; 'karyotype x *Dyrk1A*' $F_{(1,28)} = 3.877$, $p = 0.007$; **figure 3**). In the CO +/- group, knockout of a functional copy of the *Dyrk1A* gene substantially reduced the size of the cerebellum (by 10.7% vs. the CO +/+ group).

4. The sizes of the GL and the ML were normalized after the number of functional copies of the *Dyrk1A* gene was reduced in TS +/+/- mice

The thicknesses of the GL and ML were assessed to determine the mechanisms that contributed to the marked reduction in the area of the cerebellar vermis in TS +/+/+ mice and its recovery in TS +/+/- mice. The GL and ML were 11.8% and 16.8% smaller, respectively, in the TS +/+/+ mice than in the CO +/+ animals (**figures 4A**-**4C**). In addition, the cytoarchitecture of both layers was more organized in the TS +/+/- animals, in which the GL was 7.6% larger and the ML 9.6% larger than in the TS +/+/+ mice. Although these effects did not reach statistical significance (GL: ANOVA 'karyotype': $F_{(1,28)} = 0.67$, $p = 0.67$; '*Dyrk1A*': $F_{(1,28)} = 0.41$, $p = 0.52$; 'karyotype x *Dyrk1A*': $F_{(1,28)} = 7.27$, $p = 0.012$; ML: ANOVA 'karyotype': $F_{(1,28)} = 0.70$, $p = 0.40$; '*Dyrk1A*': $F_{(1,28)} = 2.44$, $p = 0.13$; 'karyotype x *Dyrk1A*': $F_{(1,28)} = 22.94$, $p < 0.001$), the sizes of the layers in the TS +/+/- mice were not different from the euploid mice.

Consistent with the reduced cerebellar size observed in CO +/- mice, the GL was 12.5% thinner and the ML was 18.9% thinner in this group than in the CO +/+ group (**figures 4A**-**4C**). Based on these results, *Dyrk1A* also plays a role in cerebellar development, and the normalization of its gene dosage in TS +/+/- mice contributed to improving the cerebellar phenotype, particularly in the ML.

5. The *Dyrk1A* copy number affects the density of GCs and Purkinje cells in the cerebellum

The cell density of the GL was analyzed to determine whether the partial recovery in the thickness of the GL observed in TS +/+/- mice was caused by an increase in the number of GCs or by changes in cellular packing. As shown in **figures 5A** and **5B**, TS +/+/+ mice displayed a markedly lower GC density ($p < 0.001$). In the TS +/+/- mice, knockout of a copy of the *Dyrk1A* gene produced a nearly complete recovery of the GC density. In addition, the CO +/- mice displayed a substantial increase in GC density compared with that of the CO +/+ group (ANOVA 'karyotype': $F_{(1,28)} = 100.582$, $p < 0.001$; '*Dyrk1A*': $F_{(1,28)} = 55.634$, $p < 0.001$; 'karyotype x *Dyrk1A*': $F_{(1,28)} = 0.044$, $p = 0.835$).

A lower linear density of Purkinje cells was observed in the TS +/+/+ than in the CO +/+ mice (**figure 6**, ANOVA 'karyotype': $F_{(1,28)} = 2.982$, $p = 0.096$). This deficit disappeared after the dosage of the *Dyrk1A* gene was normalized in TS +/+/- mice. However, the reduction in the number of functional copies of this gene in the CO +/- mice did not have any effect on the linear density of Purkinje cells (ANOVA '*Dyrk1A*': $F_{(1,28)} = 3.895$,

p = 0.059; 'karyotype x *Dyrk1A*': $F_{(1,28)} = 4.511$, p = 0.043). In contrast to GCs, Purkinje cell numbers were not affected in mice displaying a reduced cerebellar size.

6. Normalizing the dosage of the *Dyrk1A* gene restores Purkinje cell dendritic arborization in TS mice

TS +/+/+ mice displayed lower levels of Purkinje cell dendritic arborization than their CO +/+ littermates (ANOVA 'karyotype': $F_{(1,28)} = 0.046$; **figure 7**). However, the reduction in the number of copies of the *Dyrk1A* gene rescued this altered phenotype in TS +/+/- mice (ANOVA '*Dyrk1A*': $F_{(1,28)} = 4.49$, p = 0.044, **figure 7**), but did not have any effect on CO +/- mice (ANOVA 'karyotype x *Dyrk1A*': $F_{(1,28)} = 3.00$, p = 0.095).

7. Inactivating a copy of the *Dyrk1A* gene reduces the density of markers of inhibitory synapses and normalizes the density of markers of excitatory synapses in TS mice

TS mice with two or three functional copies of the *Dyrk1A* gene displayed an increased density of inhibitory synapses (karyotype': $F_{(1,28)} = 5.81$, p = 0.023; **figures 8A** and **8B**). However, knockout of the *Dyrk1A* gene had opposite effects on TS and CO mice, as it reduced the density of VGAT-positive boutons in TS mice but increased this value in CO +/- animals (ANOVA '*Dyrk1A*': $F_{(1,28)} = 0.07$, p = 0.78; 'karyotype x *Dyrk1A*': $F_{(1,28)} = 87.83$, p < 0.001; **figures 8A** and **8B**).

In addition, the density of excitatory synapses was markedly reduced in TS +/+/+ mice (ANOVA 'karyotype': $F_{(1,28)} = 30.61$, p < 0.001; **figures 8A** and **8C**). The reduction in the number of copies of the *Dyrk1A* gene in TS +/+/- and CO +/- animals increased the area occupied by VGluT1-positive boutons in both groups of mice ('*Dyrk1A*': $F_{(1,28)} = 16.55$, p < 0.001; 'karyotype x *Dyrk1A*': $F_{(1,28)} = 1.26$, p = 0.27; **figures 8A** and **8C**).

When the ratio of excitatory/inhibitory synapse markers was calculated, a marked over-inhibition was observed in the TS +/+/+ mice (ANOVA 'karyotype': $F_{(1,28)} = 12.26$, p = 0.002; **figures 8A** and **8D**) that was partially compensated for in the TS +/+/- animals. However, CO +/- mice presented a marked reduction in the ratio of excitatory/inhibitory synapse markers because they exhibited a larger increase in the area occupied by VGAT-positive boutons than the area occupied by VGluT1-positive boutons (ANOVA '*Dyrk1A*': $F_{(1,28)} = 0.39$, p = 0.53; 'karyotype x *Dyrk1A*': $F_{(1,28)} = 15.94$, p < 0.001; **figures 8A and 8D**). Thus, knocking out *Dyrk1A* partially restored the excitatory/inhibitory balance in TS +/+/- mice, but not in CO +/- animals.

8. Normalizing the *Dyrk1A* gene copy number ameliorates the altered walking pattern observed in TS mice

TS +/+/+ mice displayed an abnormal walking pattern, with a shorter stride length (ANOVA 'karyotype': $F_{(1,28)} = 5.22$, $p = 0.037$; **figure 9A**) and width ($F_{(1,28)} = 4.28$, $p = 0.05$; **figure 9B**), as well as a greater number of strides ($F_{(1,28)} = 10.77$, $p = 0.005$; **figure 9D**).

When the number of copies of the *Dyrk1A* gene was reduced by one, these deficits were ameliorated in TS +/+/- mice, but no effect was observed on CO +/- animals. The TS +/+/- group displayed a normalized stride length ('*Dyrk1A*': $F_{(1,28)} = 0.04$, $p = 0.83$; 'karyotype x *Dyrk1A*': $F_{(1,28)} = 11.62$, $p = 0.004$; **figure 9B**) and stride number ($F_{(1,28)} = 0.82$, $p = 0.38$; 'karyotype x *Dyrk1A*': $F_{(1,28)} = 8.65$, $p = 0.011$; **figure 9D**) that were similar to the values observed in CO +/+ animals. In addition, when the coefficient of variation was calculated, TS +/+/+ mice, but not TS +/+/- mice, displayed a more irregular walking pattern (ANOVA 'karyotype': $F_{(1,28)} = 0.001$, $p = 0.97$; '*Dyrk1A*': $F_{(1,28)} = 0.009$, $p = 0.92$; 'karyotype x *Dyrk1A*': $F_{(1,28)} = 9.44$, $p = 0.008$; **figure 9C**). However, normalization of the *Dyrk1A* gene copy number did not have a significant effect on the stride width of the TS +/+/- animals ('*Dyrk1A*': $F_{(1,28)} = 0.00$, $p = 0.98$; 'karyotype x *Dyrk1A*': $F_{(1,28)} = 3.17$, $p = 0.095$; **figure 9B**). These results suggest that, although *Dyrk1A* overexpression might be implicated in these deficits, other factors must also play significant roles.

DISCUSSION

The results of this study provide support for the hypothesis that *Dyrk1A* plays a role in the altered morphology of the cerebellum in a mouse model of DS. As previously demonstrated, TS +/+/+ mice possess i) a smaller cerebellar volume, ii) vermis, GL and ML sizes, in addition to iii) a reduced density of GCs and Purkinje cells. Moreover, in TS +/+/+ mice, Purkinje cells exhibit abnormal dendritic arborization, imbalanced expression of excitatory and inhibitory synaptic markers and an abnormal gait pattern. When the number of functional copies of the *Dyrk1A* gene was reduced (TS +/+/- mice), the cerebellar volume was not modified, but the sizes of the vermis, GL and ML, the density of GCs and the density and arborization of Purkinje cells were normalized, and the excitatory-inhibitory balance and abnormal walking pattern were improved.

First, high-resolution MRI revealed a reduction in the cerebellar volume in the TS +/+/+ mice than in their euploid littermates (CO +/+ mice). In addition, TS +/+/+ mice possessed a smaller cerebellar vermis, GL and ML, potentially because of changes in cell density or packaging. The results of the quantitative analysis showed reductions in the density of both GCs and Purkinje cells in TS +/+/+ mice. These results confirm those of previous studies showing marked reductions in cerebellar volume, the sizes of the vermis, GL and ML, and the densities of GCs and Purkinje cells in both murine models of DS and individuals with DS because of reductions in both the number of GC precursors and the rate of proliferation (Aylward et al., 1987; Rotmensch et al., 1997; Baxter et al., 2000; Winter et al., 2000; Olson et al., 2004; O'Doherty et al., 2005; Roper et al., 2006; Contestabile et al., 2009; Guidi et al., 2011).

Regarding cerebellar volume, knockout of a functional copy of the *Dyrk1A* gene reduced the cerebellar volume in CO +/- mice, but did not have any effect on TS +/+/- animals. *Dyrk1A* +/- haploinsufficient mice (i.e., CO +/- mice) also display smaller brains and reductions in the sizes of different CNS regions (Fotaki et al., 2002). Because of the roles of *DYRK1A/Dyrk1A* in normal brain growth in humans and mice are well established (Fotaki et al., 2002; Moeller et al., 2008; van Bon et al., 2011; Guedj et al., 2012), we predicted that normalization of its gene dosage (TS +/+/- animals) would rescue the cerebellar volume. However, these animals presented a smaller cerebellar volume than the CO +/+ mice and were not different from TS +/+/+ mice. Thus, the loss of a copy of the *Dyrk1A* gene in CO +/- mice significantly reduced their cerebellar volume, whereas normalization of the gene dosage in TS +/+/- mice did not modify this parameter. In these animals, the abnormal expression of other genes appears to play a role in the observed changes in cerebellar morphology in TS mice. In

this sense, mice that do not exhibit altered *Dyrk1A* expression but carry extra copies of the *SETD4, CBR1, CBR3, DOPEY2, MORC3, CHAF1B* and *CLDN14* genes (i.e., the 203E8-YAC mouse) display altered cerebellar morphogenesis (Rachidi et al., 2007). Thus, *Dyrk1A* overexpression seems to play a role but does not fully account for the changes in cerebellar morphology observed in TS +/+/+ mice.

Because the normalization of the *Dyrk1A* gene dosage in TS +/+/- animals rescued the size of the zones of the cerebellar cortex that were analyzed in this study (see below), *Dyrk1A* may play a role in the growth of some but not all cerebellar regions, such as the deep cerebellar nuclei, which were not evaluated in the present study. The development of the murine cerebellum is orchestrated by the interaction of multiple signaling pathways, which control the proliferation, migration and differentiation of neuronal and glial cell types. The neurogenesis of the vermis, a new evolutionary structure of mammals that is absent in other vertebrates, depends on FGF8, but the development of cerebellar lobes/hemispheres does not (Butts et al., 2014). In addition, the neuroepithelium of the IV ventricle generates all GABAergic neurons under control of the NOTCH1 and PTF1a pathway, whereas the rhombic lip, which is regulated by BMP/LMX1a signaling, is the source of glutamatergic neurons of cerebellar nuclei (Wriend et al., 2015). These pathways might be differentially affected by some of the genes overexpressed in TS +/+/+ mice, including *Dyrk1A*, leading to variations in the morphology and function of the different cerebellar structures.

The reduction in the functional copy number of the *Dyrk1A* gene normalized the sizes of the vermis, GL and ML in TS +/+/- mice and reduced their sizes in CO +/- mice. In addition, TS +/+/- mice exhibited normal GC and Purkinje cell densities. However, although the densities of some neural populations are reduced in *Dyrk1A* +/- haploinsufficient mice (Fotaki et al., 2002), GC and Purkinje cell densities were not affected in CO +/- animals. Thus, the reduced size of different cerebellar zones observed in this group of mice was not accompanied by changes in cellular packaging.

Both the density and the morphology of Purkinje cells were altered in TS +/+/+ mice. Consistent with the abnormal dendritic arborization observed in this neuronal population in the present study, Necchi et al. (2008) described morphological abnormalities in the axons of Purkinje cells. In the present study, the reduction in the functional copy number of the *Dyrk1A* gene rescued the dendritic arborization defect in TS +/+/- mouse Purkinje cells, but did not have a similar effect on CO +/- mice.

Therefore, although *Dyrk1A* seems to play a role in altering cerebellar morphology in TS mice, it is not the sole effector of this phenotype, and interactions between this gene and other genes or gene products, as well as differences in epigenetic modifications, may also contribute to some of the cerebellar alterations observed in these mice. Other genes that are triplicated in the TS mouse might play a role in the reduction in GC and Purkinje cell densities and the abnormal dendritic configuration observed in Purkinje cells. These genes include *Pcp4*, which encodes a protein expressed in Purkinje cells (PEP19) (Cabin et al., 1996; Créau et al., 2016); *SETD4, CBR1, CBR3, DOPEY2, MORC3, CHAF1B* and *CLDN14,* which play roles in cerebellar morphogenesis (Rachidi et al., 2007); and *App*, which is implicated in Purkinje cell differentiation (Ohta et al., 1993). Moreover, the Hsa21 orthologous genes that are triplicated in the TS mouse induce the aberrant expression of numerous non-Hsa21 mRNA transcripts (Saran et al., 2003). Hence, the absence of normal molecular interactions in CO +/- mice might be responsible for the different effects on cerebellar morphology observed when the copy number of the *Dyrk1A* gene was reduced by one in TS +/+/- and CO +/- mice.

The brains of TS mice are characterized by an imbalance between excitatory and inhibitory transmission (see Martínez-Cué et al., 2014). In the present study, the area of the cerebellum that expressed a marker of inhibitory synapses (VGAT) was larger and the area that expressed a marker of excitatory synapses (VGluT1) was smaller in TS +/+/+ mice. *Dyrk1A* has been reported to contribute to this imbalance. In mice with a higher dosage of *Dyrk1A*, inhibitory synapse markers occupy a larger area and excitatory synapse markers occupy a smaller area in various areas of the brain and cerebellum (García-Cerro et al., 2014; Souchet et al., 2014; 2015). In support of these findings, the reduction in the copy number of *Dyrk1A* (TS +/+/- mice) normalized the areas in the cerebellum occupied by both inhibitory and excitatory boutons. A recent study provided further support for the hypothesis that *Dyrk1A* plays a hyperinhibitory role in several areas of the brain (Souchet et al., 2015). The administration of Pol60, an extract containing the DYRK1A inhibitor epigallocatechin gallate (EGCG), restores components of excitatory/inhibitory balance in the cortex and hippocampus, but not the cerebellum, of Ts65Dn and mBACtgDyrk1a mice. The authors hypothesize that the lack of effects on this structure might be due to a reduced accessibility of the drug or to the presence of different regulatory mechanisms in the cerebellum (Souchet et al., 2015).

Although *Dyrk1A* appears to contribute to the excitatory/inhibitory imbalance observed in TS +/+/+ animals, other genes, such as *Synj1* (Voronov et al., 2008), *Olig1* and *Olig2* (Chakrabarti et al., 2010), have been shown to play important roles in this phenotype.

Finally, fine motor control is perturbed in individuals with DS (Latash and Corcos, 1991; Latash et al., 2002), and motor alterations are well established in some mouse models of DS that overexpress *Dyrk1A* (Altafaj et al., 2001). However, controversy exists regarding whether TS animals present altered motor activity. Some studies have observed altered motor coordination in TS mice (Costa et al., 1999; Gutierrez-Castellanos, 2013), whereas others have reported normal (Escorihuela et al., 1998; Baxter et al., 2000) or improved (Hyde et al., 2001) motor coordination. In the present study, we performed a more demanding version of the rotarod test (data not shown) described by Costa et al. (1999), but we did not observe any differences in motor coordination between TS +/+/+ animals and any of the other groups of mice.

However, deficits have been reported in the basic gait of TS +/+/+ animals (Costa et al., 1999). In the present study, these animals displayed an abnormal walking pattern that was characterized by a shorter stride length and width and a larger number of strides. The reduction in the copy number of the *Dyrk1A* gene (TS +/+/- mice) ameliorated these deficits but did not have a similar effect on CO +/- animals, suggesting that the structural benefits produced by normalizing the copy number of the *Dyrk1A* gene in TS mice may be partially responsible for these motor improvements.

Based on accumulating evidence, the cerebellum is involved in higher cognitive functions, including procedural learning in spatial tasks (Rondi-Reig and Burguière, 2005; Galiano et al., 2013; Rochefort et al., 2013). TS +/+/+ mice and transgenic *Dyrk1A*-overexpressing mice exhibit severe impairments in these cognitive domains (Smith et al., 1997; Altafaj et al., 2001; Ahn et al., 2006; Bartesaghi et al., 2011). Pharmacological manipulations that normalize cerebellar morphology in TS +/+/+ mice improve spatial learning and memory (Das et al. 2013), suggesting that the cerebellar hypoplasia observed in trisomic animals may contribute to some of their cognitive deficits.

In summary, the *Dyrk1A* gene is involved in several of the morphological and functional cerebellar phenotypes observed in TS mice. However, normalization of the *Dyrk1A* gene dosage did not fully restore the cerebellar volume and only partially ameliorated

the altered walking pattern observed in these mice, suggesting that other genes or gene products are implicated in these cerebellar anomalies.

Conflict of interests: The authors have no competing financial interests to declare.

Acknowledgements: This work was supported by grants from the Jerome Lejeune Foundation and Fundación Tatiana Pérez de Guzmán el Bueno and the Spanish Ministry of Economy and Competitiveness (PSI-2016-76194-R, AEI/FEDER, EU) and "Centro de Investigación Biomédica en Red sobre Enfermedades Neurodegenerativas (CIBERNED, CB06/05/0037)" from Spain. The authors wish to express their gratitude to Mariona Arbonés for providing the *Dyrk1A*+/- KO mice, to Eva García Iglesias for providing technical assistance, to Juan Mendizabal-Zubiaga and Fernando Calvo Baltanás for providing technical advice and the anti-calbindin antibody and to Victor Campa for the advices in the acquisition and processing of the microscopy images.

REFERENCES

Abercrombie M (1946) Estimation of nuclear population from microtome sections. Anat Rec 94:239-247.

Ahn KJ, Jeong HK, Choi HS, Ryoo SR, Kim YJ, Goo JS, Choi SY, Han JS, Ha I, Song WJ (2006) DYRK1A BAC transgenic mice show altered synaptic plasticity with learning and memory defects. Neurobiol Dis 22:463-472.

Altafaj X, Dierssen M, Baamonde C, Martí E, Visa J, Guimerà J, Oset M, González JR, Flórez J, Fillat C, Estivill X (2001) Neurodevelopmental delay, motor abnormalities and cognitive deficits in transgenic mice overexpressing Dyrk1A (minibrain), a murine model of Down's syndrome. Hum Mol Genet 10:1915-23.

Aylward EH, Habbak R, Warren AC, Pulsifer MB, Barta PE, Jerram M, Pearlson GD (1997) Cerebellar volume in adults with Down syndrome. Arch Neurol 54:209-212.

Bartesaghi R, Guidi S, Ciani E. (2011) Is it possible to improve neurodevelopmental abnormalities in Down syndrome? Reviews in the Neurosciences 22: 419–455.

Baxter LL, Moran TH, Richtsmeier JT, Troncoso J, Reeves RH (2000) Discovery and genetic localization of Down syndrome cerebellar phenotypes using the Ts65Dn mouse. Hum Mol Genet 9:195-202.

Becker W, Sippl W (2011) Activation, regulation, and inhibition of DYRK1A. FEBS J 278: 246-256.

Bowes C, Li T, Frankel WN, Danciger M, Coffin JM, Applebury ML, Farber DB (1993) Localization of a retroviral element within the rd gene coding for the beta subunit of cGMP phosphodiesterase. Proc Natl Acad Sci USA 90: 2955-2959.

Butts T, Green MJ, Wingate R.J.T. (2014) Development of the cerebellum: simple steps to make a “Little brain”. Development 141:4031-4041.

Cabin DE, Gardiner K, Reeves RH (1996) Molecular genetic characterization and comparative mapping of the human PCP4 gene. Somat Cell Mol Genet 22:167-175.

Chakrabarti L, Best TK, Cramer NP, Carney RS, Isaac JT, Galdzicki Z, Haydar TF (2010) Olig1 and Olig2 triplication causes developmental brain defects in Down syndrome. Nat Neurosci 13:927-934.

Contestabile A, Fila T, Bartesaghi R, Ciani E (2009) Cell cycle elongation impairs proliferation of cerebellar granule cell precursors in the Ts65Dn mouse, an animal model for Down syndrome. Brain Pathol 19:224-237.

Costa AC, Walsh K, Davisson MT (1999) Motor dysfunction in a mouse model for Down syndrome. Physiol Behav 68:211-220.

Créau N, Cabet E, Daubigney F, Souchet B, Bennaï S, Delabar J (2016) Specific age-related molecular alterations in the cerebellum of Down syndrome mouse models. Brain Res 1646:342-353.

Das I, Park J-M, Shin JH, Jeon SK, Lorenzi H, Linden DJ, Worley PF, Reeves RH (2013) Hedgehog agonist therapy corrects structural and cognitive deficits in a Down syndrome mouse model. Science Tranlational Medicine 5: 201ra120.

Escorihuela RM, Vallina IF, Martínez-Cué C, Baamonde C, Dierssen M, Tobeña A, Flórez J, Fernández-Teruel A (1993) Impaired short- and long-term memory in Ts65Dn mice, a model for Down syndrome. Neurosci Lett 247:171-174.

Fotaki V, Martínez De Lagrán M, Estivill X, Arbonés M, Dierssen M (2004) Haploinsufficiency of Dyrk1A in mice leads to specific alterations in the development and regulation of motor activity. Behav Neurosci 118: 815-821.

Fotaki V, Dierssen M, Alcántara S, Martínez S, Martí E, Casas C, Visa J, Soriano E, Estivill X, Arbonés ML (2002) Dyrk1A haploinsufficiency affects viability and casues developmental delay and abnormal brain morphology in mice. Mol Cell Biol 22: 6636-6647.

Galiano E, Gao Z, Schonewille M, Todorov B, Simons E, Pop AS, D'Angelo E, van den Maagdenberg AMJM, Hoebeek FE, De Zeeuw CI (2013) Silencing the majority of cerebellar granule cells uncovers their essential role in motor learning and consolidation. Cell Reports 3: 1239-1251.

García-Cerro S, Martínez P, Vidal V, Corrales A, Flórez J, Vidal R, Rueda N, Arbonés ML, Martínez-Cué C (2014) Overexpression of Dyrk1A is implicated in several cognitive, electrophysiological and neuromorphological alterations found in a mouse model of Down syndrome. PLoS One 9:e106572.

Guedj F, Lopes Pereira P, Najas S, Barallobre M-J, Chabert C, Souchet B, Sebrie C, Verney C, Herault Y, Arbonés M, Delabar JM (2012) DYRK1A: A master regulatory protein controlling brain growth. Neurobiol Dis 46: 190-203.

Guidi S, Ciani E, Bonasoni P, Santini D, Bartesaghi R (2011) Widespread proliferation impairment and hypocellularity in the cerebellum of fetuses with down syndrome. Brain Pathol 21:361-373.

Gutierrez-Castellanos N, Winkelman BHJ, Tolosa-Rodriguez L, Devenney B, Reeves RH, De Zeeuw CI. Size does not always matter: Ts65Dn Down syndrome mice show cerebellum-dependent motor learning deficits that cannot be rescued by postnatal SAG treatment (2013) The Journal of Neuroscience 33: 15408-15413.

Hilber P, Jouen F, Delhaye-Bouchaud N, Mariani J, Caston J (1998) Differential roles of cerebellar cortex and deep cerebellar nuclei in learning and retention of a spatial task: studies in intact and cerebellectomized lurcher mutant mice. Behav Genet 28: 299-308.

Hyde LA, Crnic LS, Pollock A, Bickford PC (2001) Motor learning in Ts65Dn mice, a model for Down syndrome. Dev Psychobiol 38:33-45.

Latash ML, Kang N, Patterson D (2002) Finger coordination in persons with Down syndrome: atypical patterns of coordination and the effects of practice. Exp Brain Res 146, 345–355.

Liu DP, Schmidt C, Billings T, Davisson MT (2003) A quantitative PCR genotyping assay for the Ts65Dn mouse model of Down syndrome. Biotechniques 35: 1170-1174.

Lowry OH, Rosenbrough NJ, Farr AL, Randall RJ (1951) Protein measurement with the Folin phenol reagent. J Biol Chem 193: 265-275.

Martí E, Altafaj X, Dierssen M, de la Luna S, Fotaki V, Alvarez M, Pérez-Riba M, Ferrer I, Estivill X (2003) Dyrk1A expression pattern supports specific roles of this kinase in the adult central nervous system. Brain Res 964:250-263.

Martínez-Cué C, Delatour B, Potier MC (2014) Treating enhanced GABAergic inhibition in Down syndrome: use of GABA α5-selective inverse agonists. Neurosci Biobehav Rev 46 Pt 2:218-227.

Martínez-Cué C, Martínez P, Rueda N, Vidal R, García S, Vidal V, Corrales A, Montero JA, Pazos A, Flórez J, Gasser R, Thomas AW, Honer M, Knoflach F, Trejo JL, Wettstein JG, Hernandez MC (2013) Reducing GABAA α5 receptor-mediated inhibition rescues functional and neuromorphological deficits in a mouse model of Down syndrome. J Neurosci 33: 3953-3966.

Martínez de Lagrán M, Altafaj X, Gallego X, Martí E, Estivill X, Sahún I, Fillat C, Dierssen M (2004) Motor phenotypic alterations in TgDyrk1a transgenic mice implicate DYRK1A in Down syndrome motor dysfunction. Neurobiol Dis 15:132-142.

Moeller RS, Kübart S, Hoeltzenbein M, Heye B, Vogel I, Hansen CP, Menzel C, Ullmann R, Tommerup N, Ropers HH, Tümer Z, Kalscheuer VM (2008) Truncation of the Down syndrome candidate gene DYRK1A in two unrelated patients with microcephaly. Am J Hum Genet 82: 1165-1170.

Necchi D, Lomoio S, Scherini E (2008) Axonal abnormalities in cerebellar Purkinje cells of the Ts65Dn mouse. Brain Res 1238:181-188.

O'Doherty A, Ruf S, Mulligan C, Hildreth V, Errington ML, Cooke S, Sesay A, Modino S, Vanes L, Hernandez D, Linehan JM, Sharpe PT, Brandner S, Bliss TV, Henderson DJ, Nizetic D, Tybulewicz VL, Fisher EM (2005) An aneuploid mouse strain carrying human chromosome 21 with Down syndrome phenotypes. Science 309:2033-2037.

Ohta M, Kitamoto T, Iwaki T, Ohgami T, Fukui M, Tateishi J (1993) Immunohistochemical distribution of amyloid precursor protein during normal rat development. Brain Res Dev Brain Res 75:151-61.

Olson LE, Roper RJ, Baxter LL, Carlson EJ, Epstein CJ, Reeves RH (2004) Down syndrome mouse models Ts65Dn, Ts1Cje, and Ms1Cje/Ts65Dn exhibit variable severity of cerebellar phenotypes. Dev Dyn. 2004; 230:581-589.

Palay SL, Chan-Palay V (1982) The Cerebellum. New Vistas. Springer-Verlag, Berlin.

Petrosini L, Leggio MG, Molinari M (1998) The cerebellum in the spatial problem solving: a co-star or a guest star? Prog Neurobiol 56:191-210.

Rachidi M, Lopes C, Vayssettes C, Smith DJ, Rubin EM, Delabar J-M (2007) New cerebellar phenotypes in YAC transgenic mouse in vivo library of human Down syndrome critical region-1. Biochemical and Biophysical Research Communications 364: 488-494.

Rochefort C, Lefort JM, Rondi-Reig L (2013) The cerebellum: a new key structure in the navigation system. Frontiers in Neural Circuits 7: 1-12.

Rondi-Reig L, Burguière E (2005) Is the cerebellum ready for navigation? Prog Brain Res 148:199-212.

Roper RJ, Baxter LL, Saran NG, Klinedinst DK, Beachy PA, Reeves RH (2006) Defective cerebellar response to mitogenic Hedgehog signaling in Down syndrome mice. Proc Natl Acad Sci U S A 103:1452-6.

Rotmensch S, Goldstein I, Liberati M, Shalev J, Ben-Rafael Z, Copel JA (1997) Fetal transcerebellar diameter in Down syndrome. Obstet Gynecol 89:534–537.

Sago H, Carlson EJ, Smith DJ, Kilbridge J, Rubin EM, Mobley WC, Epstein CJ, Huang TT (1998) Ts1Cje, a partial trisomy 16 mouse model for Down syndrome, exhibits learning and behavioral abnormalities.Proc Natl Acad Sci U S A. 95:6256-61.

Saran NG, Pletcher MT, Natale JA, Cheng Y, Reeves RH (2003) Global disruption of the cerebellar transcriptome in a Down syndrome mouse model. Human Molecular Genetics 12: 2013-2019.

Smith DJ, Stevens ME, Sudanagunta SP, Bronson RT, Makhinson M, Watabe AM, O'Dell TJ, Fung J, Weier HU, Cheng JF, Rubin EM (1997) Functional screening of 2 Mb of human chromosome 21q22.2 in transgenic mice implicates minibrain in learning defects associated with Down syndrome. Nat Genet 16:28-36.

Souchet B, Guedj F, Penke-Verdier Z, Daubigney F, Duchon A, Herault Y, Bizot JC, Janel N, Créau N, Delatour B, Delabar JM (2015) Pharmacological correction of excitation/inhibition imbalance in Down syndrome mouse models. Front Behav Neurosci 9:267.

Souchet B, Guedj F, Sahún I, Duchon A, Daubigney F, Badel A, Yanagawa Y, Barallobre MJ, Dierssen M, Yu E, Herault Y, Arbones M, Janel N, Créau N, Delabar JM (2014) Excitation/inhibition balance and learning are modified by Dyrk1a gene dosage. Neurobiol Dis 69:65-75.

Sturgeon X, Gardiner KJ (2011) Transcript catalogs of human chromosome 21 and orthologous chimpanzee and mouse regions. Mammalian Genome 22:261–271.

Tejedor FJ, Hämmerle B (2011) MNB/DYRK1A as a multiple regulator of neuronal development. FEBS J 278: 223-235.

van Bon BW, Hoischen A, Hehir-Kwa J, de Brouwer AP, Ruivenkamp C, Gijsbers AC, Marcelis CL, de Leeuw N, Veltman JA, Brunner HG, de Vries BB (2011) Intragenic deletion in DYRK1A leads to mental retardation and primary microcephaly. Clin Genet 79: 296-299.

Voronov SV, Frere SG, Giovedi S, Pollina EA, Borel C, Zhang H, Schmidt C, Akeson EC, Wenk MR, Cimasoni L, Arancio O, Davisson MT, Antonarakis SE, Gardiner K, De Camilli P, Di Paolo G (2008) Synaptojanin 1-linked phosphoinositide dyshomeostasis and cognitive deficits in mouse models of Down's syndrome.Proc Natl Acad Sci U S A 105:9415-9420.

Wriend J, Ghavami S, Marzban H (2015) The role of the ubiquitin proteasome system in cerebellar development and medulloblastoma. Molecular Brain 8:64

Winter TC, Ostrovsky AA, Komarniski CA, Uhrich SB (2000) Cerebellar and frontal lobe hypoplasia in fetuses with trisomy 21: usefulness as combined US markers. Radiology 214:533–538.

FIGURE CAPTIONS

Figure 1. Normalization of the copy number of the *Dyrk1A* gene reduced levels of the Dyrk1A protein in the cerebellum of TS and CO mice. Representative images and western blot analysis of the levels of the Dyrk1A protein in the cerebellum of CO +/+, CO +/-, TS +/+/+ and TS +/+/- mice. Differences between CO +/-, TS +/+/+ and +/+/- animals are expressed relative to the values observed in CO (+/+) mice (defined as 100%) (B). GAPDH was used as an internal loading control. **: $p < 0.01$ TS +/+/+ vs. CO +/+; #: $p < 0.01$ TS +/+/+ vs. TS +/+/- or CO +/+ vs. CO +/- (n = 24 in B). Significance was determined using ANOVAs and Bonferroni's post hoc test.

Figure 2. Normalization of the *Dyrk1A* gene dosage did not rescue the reduced cerebellar volume observed in TS +/+/- mice. Representative MRIs of the horizontal, sagittal and coronal planes of the four groups of mice. The scale bar corresponds to 1 mm (A). Means ± S.E.M. of the percentage differences in the cerebellar volume between TS +/+/+, TS +/- and CO +/- mice and CO +/+ mice (100%) (B). ***: $p < 0.001$ TS +/+/+ vs. CO +/+ Student's t-test; ###: $p < 0.001$ CO +/- vs. CO +/+ (n = 40 in B). Significance was determined using ANOVAs and Bonferroni's post hoc test.

Figure 3. Normalization of the *Dyrk1A* gene dosage rescued the size of the cerebellar vermis in TS +/+/- mice. Representative photographs of the cerebellar vermis of the four groups of mice. Tissues were stained with DAPI. The scale bar corresponds to 200 µm (A). Means ± S.E.M. of the percentage differences in the sizes of the cerebellar vermis between each experimental group and the CO +/+ group (100%) (B). **: $p < 0.01$, TS +/+/+ vs. CO +/+; #: $p < 0.05$, CO +/+ vs. CO +/- (n = 32 in B). Significance was determined using ANOVAs and Bonferroni's post hoc test.

Figure 4. Normalization of the ***Dyrk1A* gene dosage partially restored the cerebellar architecture in TS +/+/- mice.** Representative images of sections of the GL and ML, which are separated by the Purkinje cell layer (PL), in the four groups of animals. Sections were stained using DAPI. The white dotted line indicates the end of the ML. The scale bar corresponds to 50 µm (A). Means ± S.E.M. of the percentage differences in the thickness of the GL (B) and ML (C) compared to those of CO +/+ mice. **: $p < 0.01$, ***: $p < 0.001$ TS +/+/+ vs. CO +/+; ##: $p < 0.01$, ###: $p < 0.001$, CO +/+ vs. CO +/- (n = 32 in B and C). Significance was determined ANOVAs and Bonferroni's post hoc test.

Figure 5. **Normalization of the *Dyrk1A* gene dosage restored the density of GCs in TS mice.** Representative images of GCs stained with DAPI. The scale bar corresponds to 10 µm (A). Means ± S.E.M. of the estimated densities of GCs in each group (B). ***: $p < 0.001$, TS +/+/+ vs. CO +/+; ###: $p < 0.001$, CO +/+ vs. CO +/- and TS +/+/+ vs. TS +/+/- (n = 32 in B). Significance was determined using ANOVAs and Bonferroni's post hoc test.

Figure 6. Normalization of the *Dyrk1A* gene dosage restored the density of Purkinje cells in the cerebellum in TS mice. Representative images of Purkinje cells stained with DAPI and PI (A). Means ± S.E.M. of the estimated densities of Purkinje cells in each experimental group (B). **: $p < 0.01$ TS +/+/+ vs. CO +/+; #: $p < 0.05$ CO +/+ vs. CO +/- (n = 32 in B). Significance was determined using ANOVAs and Bonferroni's post hoc test.

Figure 7. Normalization of the *Dyrk1A* gene dosage restored the dendritic arborization of Purkinje cells in TS mice. Representative images of calbindin immunostaining in cerebellar slices of the four groups of animals. The scale bar represents 50 µm (A). Means ± S.E.M. of the densities of calbindin-stained cells in CO

+/+, CO +/-, TS +/+/+ and TS +/+/- mice. *: $p < 0.05$ TS +/+/+ vs. CO +/+; ##: $p < 0.01$ TS +/+/+ vs. TS +/+/- (n = 32 in B). Significance was determined using ANOVAs and Bonferroni's post hoc tests.

Figure 8. **Normalization of the copy number of the *Dyrk1A* gene reduced the density GABAergic synapse markers and increased the density of glutamatergic synapse markers in the cerebellum of TS mice.** Representative confocal images of sections immunostained for VGAT, VGluT1 and both VGAT and VGluT1. The scale bar represents 5 µm (A). Means ± SEM of the percentage of area occupied by VGAT-positive (B), and VGluT1-positive boutons (C) and the ratio (D) of these areas in the cerebellum of TS +/+/+, TS +/+/-, CO +/+ and CO +/- mice. **: $p < 0.01$, ***: $p < 0.001$ TS +/+/+ vs. CO +/+; #: $p < 0.05$, ##: $p < 0.01$, ###: $p < 0.001$ TS +/+/+ vs. TS +/+/- (n = 32 in B, C and D). Significance was determined using ANOVAs and Bonferroni's post hoc tests.

Figure 9. **Normalization of the *Dyrk1A* copy number reduced alterations in the walking pattern of TS mice.** Means ± S.E.M. of stride length (A), stride width (B), the coefficient of variation (C) and the number of strides (D) in TS +/+/+, TS +/+/-, CO +/+ and CO +/- mice. Representative images of the walking pattern of an animal from each group (E). *: $p < 0.05$, **: $p < 0.01$ TS +/+/+ vs. CO +/+; #: $p < 0.05$, ##: $p < 0.01$ TS +/+/+ vs. TS +/+/- (n = 32 in A, B, C and D). Significance was determined using ANOVAs and Bonferroni's post hoc tests.

Figure 1

A.

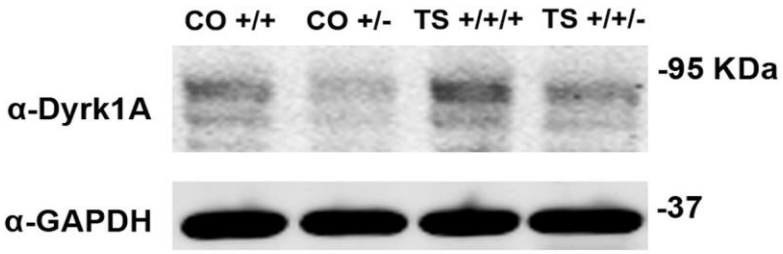

B.

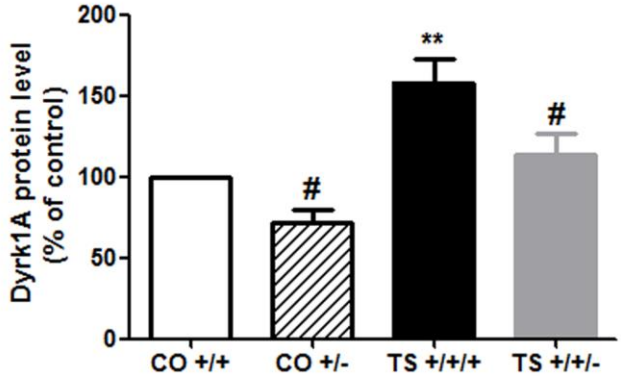

Figure 2

A.

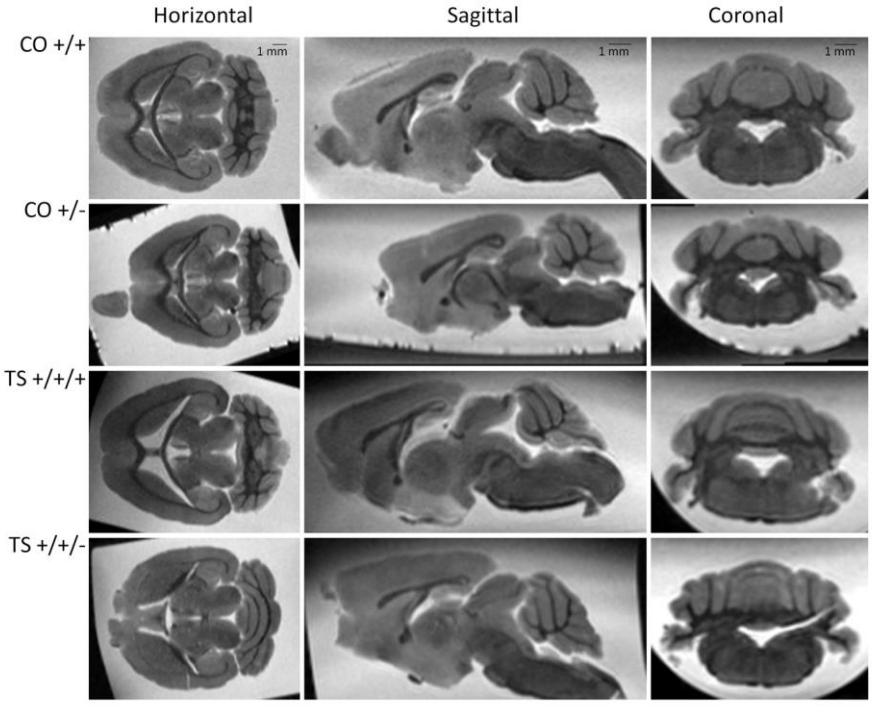

B.

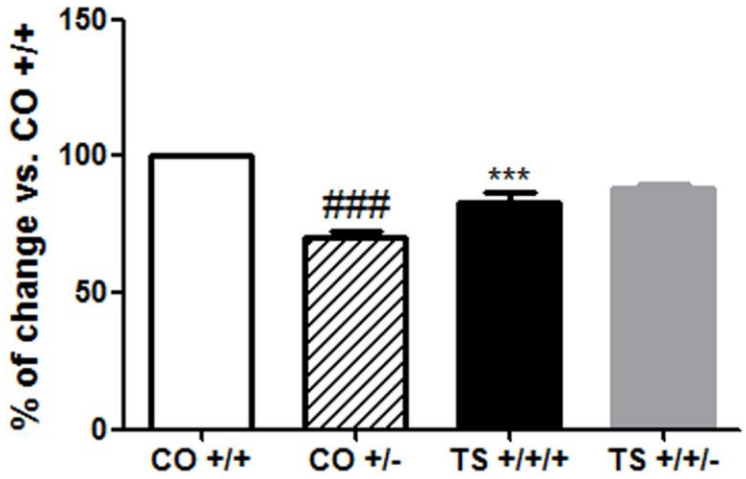

Figure 3

A.

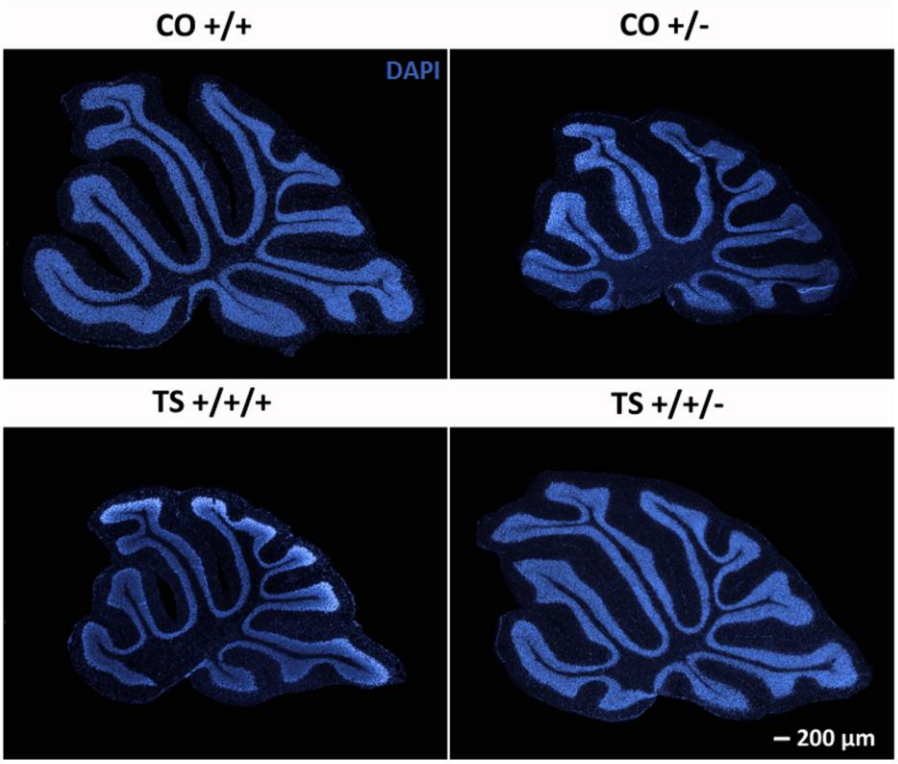

B.

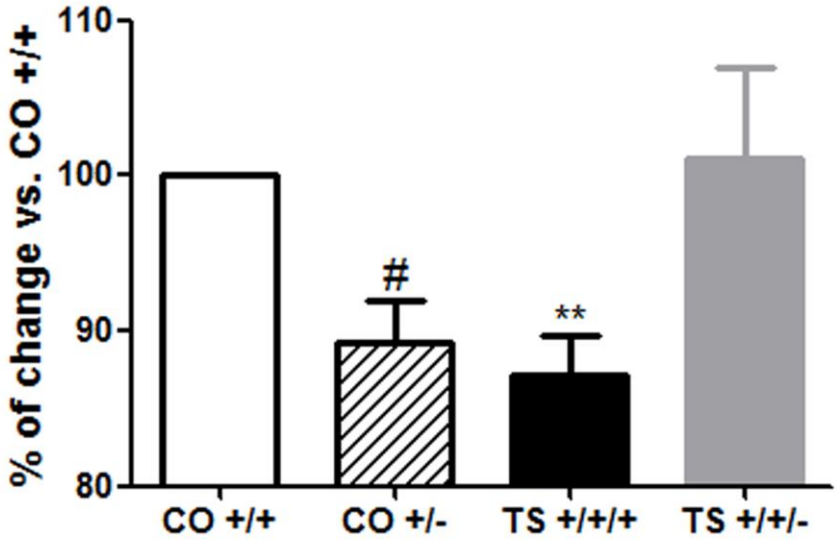

Figure 4

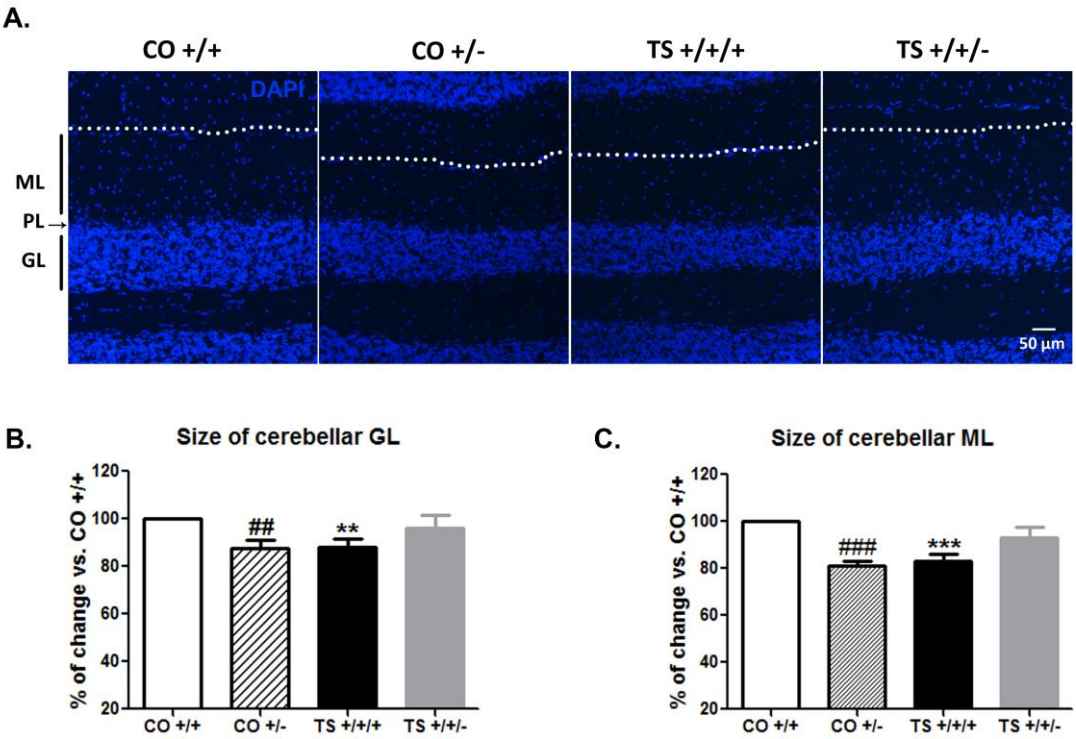

Figure 5

A.

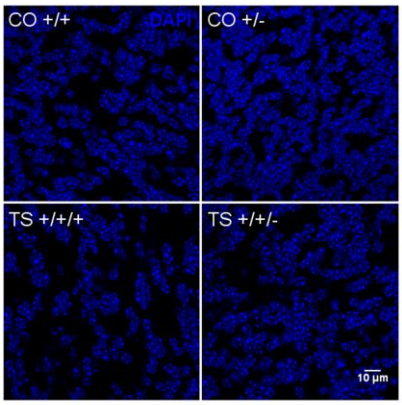

B.

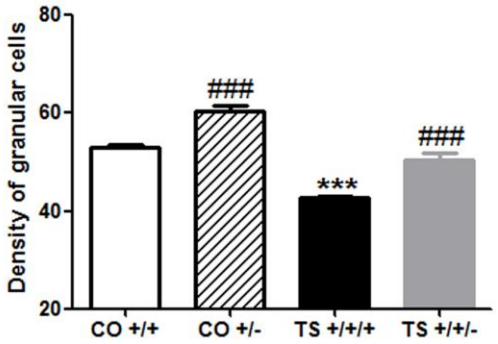

Figure 6

A.

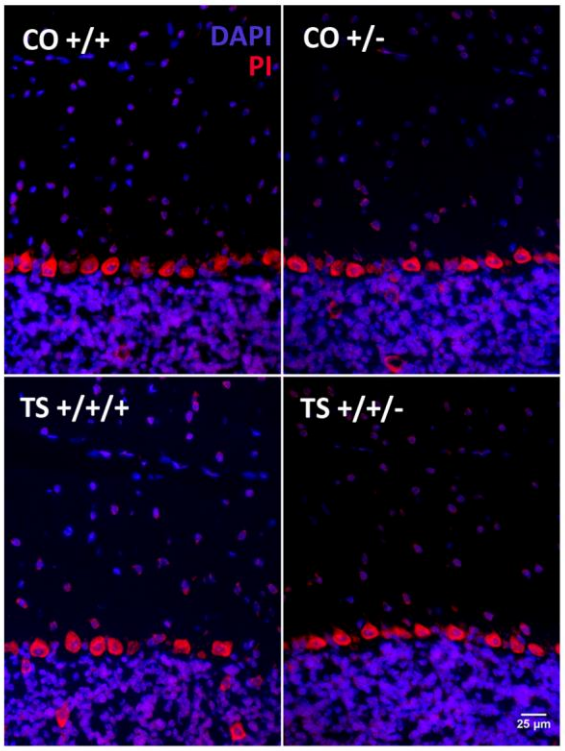

B.

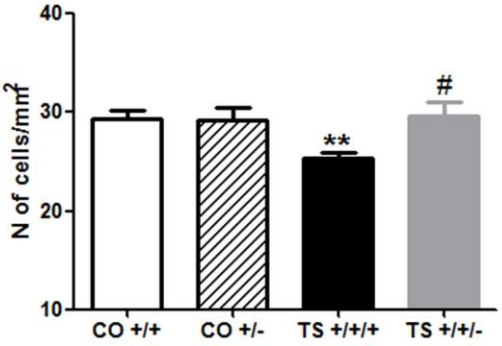

Figure 7

A.

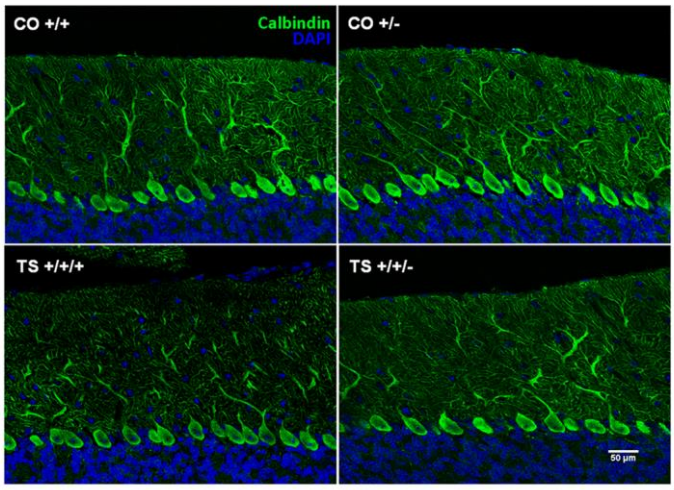

B.

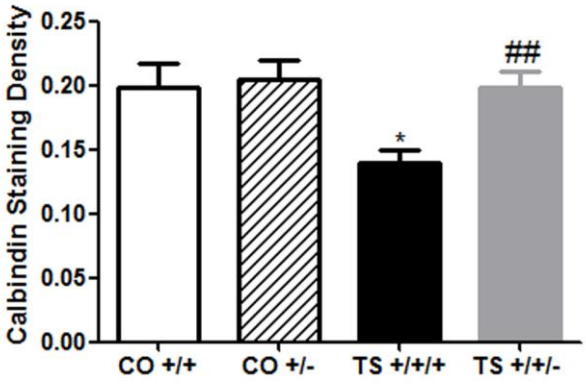

Figure 8

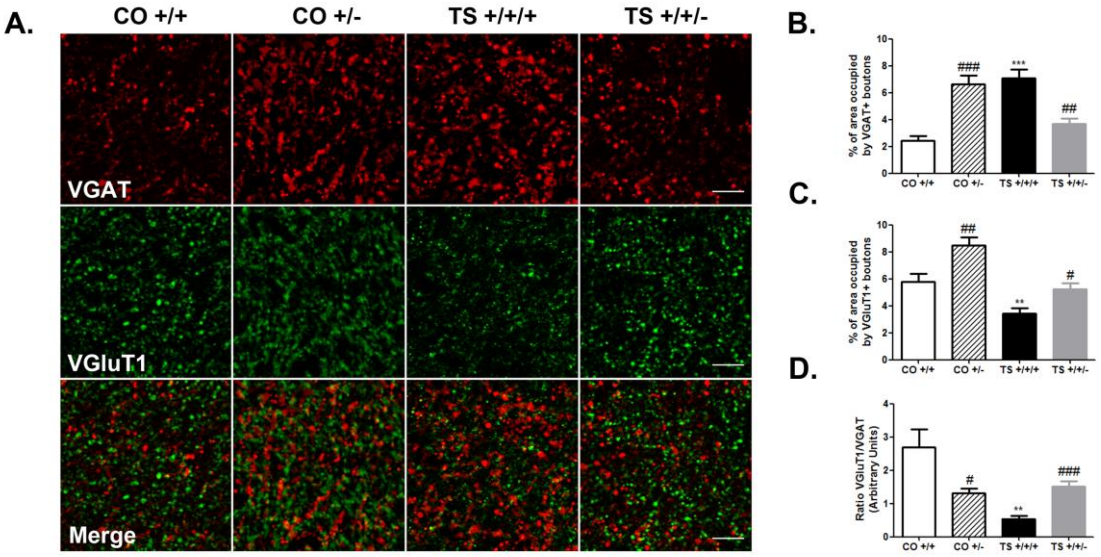

Figure 9